Annals of Diagnostic Pathology 57 (2022) 151885

Contents lists available at ScienceDirect

Annals of Diagnostic Pathology

journal homepage: www.elsevier.com/locate/anndiagpath

Original Contribution

# Infantile fibrosarcoma with an *EGFR kinase domain duplication*: Underlining a close relationship with congenital mesoblastic nephroma and highlighting a similar morphological spectrum

R. van Spronsen [a,1], L.A. Kester [a,1], R.R.G. Knops [a], M.A.J. van de Sande [a,b], G.J.L. H. van Leenders [c], P.C.J. de Laat [d], E. Stortelder [a], E. Korpershoek [c], M.M. van Noesel [a,e], M. T. Meister [a], M.J.A. Groot Koerkamp [a], N. de Graaf [f], I. Giovannoni [g], B.B.J. Tops [a], R. R. de Krijger [a,h], S.A.J. ter Horst [a,i], U. Flucke [a,j], R. Alaggio [g,1], L.S. Hiemcke-Jiwa [a,*,1]

[a] *Princess Máxima Center for Pediatric Oncology, Utrecht, the Netherlands*
[b] *Department of Orthopedic surgery, Leiden University Medical Center, Leiden, the Netherlands*
[c] *Department of Pathology, Erasmus MC Cancer Institute, University Medical Centre, Rotterdam, the Netherlands*
[d] *Department of Pediatric Oncology, Erasmus Medical Center, Rotterdam, the Netherlands*
[e] *Division Imaging & Cancer, University Medical Center Utrecht, the Netherlands*
[f] *Department of Radiology & Nuclear medicine, Erasmus MC University Medical Centre, Rotterdam, the Netherlands*
[g] *Pathology Unit, Department of Laboratories, Bambino Gesù Children's Hospital, IRCCS, Rome, Italy*
[h] *Department of Pathology, University Medical Center Utrecht, Utrecht, the Netherlands*
[i] *Department of Radiology, University Medical Center Utrecht, Utrecht, the Netherlands*
[j] *Department of Pathology, Radboud University Medical Center, Nijmegen, the Netherlands*

ARTICLE INFO

*Keywords:*
Infantile fibrosarcoma
Congenital mesoblastic nephroma
EGFR kinase domain duplication
RNA sequencing

ABSTRACT

Infantile fibrosarcoma (IFS) and congenital mesoblastic nephroma (CMN) are locally aggressive tumors primarily occurring in infants. Both IFS and the cellular subtype of CMN show overlapping morphological features and an *ETV6-NTRK3* fusion, suggesting a close relationship. An activating alteration of EGFR, based on an *EGFR kinase domain duplication* (*KDD*), occurs in a subset of CMNs lacking an *NTRK3* rearrangement, especially in the classic and mixed type. So far no *EGFR-KDDs* have been detected in IFS.

We describe four pediatric tumors at the extremities (leg, $n = 2$; foot and arm $n = 1$) with histological features of IFS/CMN. Two cases showed classic IFS morphology while two were similar to classic/mixed type CMN. In all cases, an *EGFR-KDD* was identified without detection of a fusion gene. There were no abnormalities of the kidneys in any of the patients.

This is the first description of IFS with an *EGFR-KDD* as driver mutation, supporting that IFS and CMN are similar lesions with the same morphological and genetic spectrum. Pathologists should be aware of the more fibrous variant of IFS, similar to classic/mixed type CMN. Molecular analyses are crucial to treat these lesions adequately, especially with regard to the administration of tyrosine kinase inhibitors.

## 1. Introduction

Infantile fibrosarcoma (IFS) is a malignant (myo)fibroblastic tumor of infancy, most often with locally aggressive behavior and metastases occurring only rarely [1-4]. Prognosis tends to be good, with a 5-year overall survival of nearly 90% [2-5]. Complete resection is the treatment of choice. However, in case of large tumor size or the need for invasive or even ablative surgery, induction chemotherapy is used to reduce tumor size and minimalize mutilating surgery [1,6]. As over 90% of IFSs carry an *ETV6-NTRK3* fusion [5], NTRK inhibitors have recently shown great therapeutic potential for patients with an IFS in phase 1 and 2 clinical trials, and NTRK inhibitors are quickly replacing the role of chemotherapy [7,8].

Congenital mesoblastic nephroma (CMN) is a mesenchymal renal

* Corresponding author at: Princess Máxima Center for Pediatric Oncology, Heidelberglaan 100, 3584 CX Utrecht, the Netherlands.
*E-mail address:* L.S.Jiwa-3@prinsesmaximacentrum.nl (L.S. Hiemcke-Jiwa).
[1] Authors contributed equally.

https://doi.org/10.1016/j.anndiagpath.2021.151885

Available online 3 January 2022

tumor, generally occurring within the first three months of life. Prognosis is commonly excellent with radical resection being the primary choice for treatment [2,9]. Worse outcome, however rare, has mainly been reported in the cellular subtype [2,10]. Originally, CMNs were characterized by low cellularity, but further research also unveiled more cellular and mitotically active CMNs, some of which even contained necrosis. Consequently, the hypocellular subtype is referred to as classic, while cases with the more sarcoma-like appearance are termed cellular (cCMN). The mixed subtype contains both patterns [11-16].

cCMN shows striking clinicopathological similarities with IFS and is also characterized by an *ETV6-NTRK3* fusion [11,17]. Therefore, it has been suggested that IFS represents the soft tissue counterpart of cCMN [11,18-20]. A subset of CMN cases lacking an *NTRK3* rearrangement carry *EGFR* alterations instead, mostly a *kinase domain duplication* (*KDD*) and rarely splice site mutations. *EGFR-KDD* is an in-frame tandem duplication of exons 18–25 which encodes the entire tyrosine kinase domain of the EGFR protein leading to a duplication of the tyrosine kinase domain and an EGFR activating configuration [19]. This *EGFR-KDD* has been identified in the majority of classic and mixed CMNs and rarely in the cellular subtype [21,22]. Intriguingly, as of yet no *EGFR-KDDs* have been described in IFS [22].

In this case series we describe four pediatric tumors located at the extremities, clinically and morphologically resembling IFS/CMN, all harboring an *EGFR-KDD*.

## 2. Materials and methods

The cases were retrieved from the author's registries. Besides the four IFS cases, two fusion-negative CMNs (one mixed type and one cCMN) were included as control cases. In all cases, the tissue was fixed in 4% buffered formalin, routinely processed and embedded in paraffin (FFPE); 4 μm thick sections were stained with hematoxylin and eosin. In addition, fresh frozen tissue was stored for molecular analyses.

### 2.1. Immunohistochemistry

Four μm thick sections from FFPE blocks were cut, mounted on precoated slides and dried for at least 10 min at 56 °C. After deparaffinization the slides were stained using an automated Ventana tissue stainer (BenchMark Ultra, Roche). The following antibodies were used: pan-TRK, Abcam, clone EPR17341, 1:500, and EGFR, Invitrogen, clone 21G7, 1:40. For pretreatment of the pan-TRK antibody, slides were cooked in EDTA for 24 min and then incubated for 32 min. For pretreatment of the EGFR antibody, slides were incubated with Protease 1 for 8 min and incubated for 32 min. For EGFR, incubation with the secondary antibody was followed by an amplification step for 8 min.

### 2.2. Next generations sequencing

Next generations sequencing (NGS) was performed as previously described [23].

### 2.3. Whole transcriptome sequencing (WTS) (cases 1–3)

WTS was performed as previously described [24]. In short: total RNA was isolated using the AllPrep DNA/RNA/Protein Mini Kit (QIAGEN) according to standard protocol on the QiaCube (Qiagen). RNA-seq libraries were generated with 300 ng RNA using the KAPA RNA HyperPrep Kit with RiboErase (Roche) and subsequently sequenced on a NovaSeq 6000 system (2 × 150 bp) (Illumina). The RNA sequencing data were processed as per the GATK 4.0 best practices workflow for variant calling, using a wdl and cromwell based workflow (https://gatk.broadinstitute.org/hc/en-us/sections/360007226651-Best-Practices-Workflows). This included performing quality control with Fastqc (version 0.11.5) to calculate the number of sequencing reads and the insert size Picard (version 2.20.1) for RNA metrics output and MarkDuplicates [25]. The raw sequencing reads were aligned using Star (version 2.7.0f) to GRCh38 and gencode version 29 [26]. Finally, expression counts were determined at gene level using Subread Counts [27].

### 2.4. Gene expression analysis

Gene expression profiles of these cases were compared to all other samples for which RNA sequencing data were available within the Princess Maxima Center, Utrecht, The Netherlands. Comparison was done based on a k-nearest neighbor algorithm using the first 100 principal components derived from the 5000 most differentially expressed genes across all samples. The classification score is based on the majority vote of 100 different models, each built with a different subset of the total dataset. Scores range between 0 and 1, with 1 being the most confident score for the suggested diagnosis.

### 2.5. Whole exome sequencing (WES) (cases 1–3)

Total DNA was isolated using the AllPrep DNA/RNA/Protein Mini Kit (QIAGEN) according to standard protocol on the QiaCube (Qiagen). DNA-seq libraries were generated with 150 ng DNA using the KAPA HyperPrep Kit in combination with the HyperExome capture kit (Roche) and subsequently sequenced on a NovaSeq 6000 system (2 × 150 bp) (Illumina). The DNA sequencing data of the tumor and the normal DNA (extracted from blood) were processed as per the GATK 4.0 best practices workflow for variant calling, using a wdl and cromwell based workflow (https://gatk.broadinstitute.org/hc/en-us/sections/360007226651-Best-Practices-Workflows). This included performing quality control with Fastqc (version 0.11.5) to calculate the number of sequencing reads and the insert size Picard (version 2.20.1) for DNA metrics output and MarkDuplicates [25].

## 3. Results

### 3.1. Clinical and radiological characteristics

#### 3.1.1. Case 1

A girl was born with a rapidly growing large swelling of 11.3 cm on her anterior right lower leg. The overlying skin showed purple discoloration with ulceration (Fig. 1). MRI revealed a corresponding large mass predominantly in the skin and subcutaneous fat. The mass was strongly heterogeneous with solid and cystic components and hemorrhages (Fig. 1). No other abnormalities, especially of the kidneys, were detected by ultrasound and chest CT-scan.

The patient responded well to the standard vincristine-actinomycin-D chemotherapy with significant decrease of tumor size [5]. After 8 months of chemotherapy treatment the tumor was completely resected showing profound regressive changes with 20–30% remaining vital tumor. The patient is currently in follow-up.

#### 3.1.2. Case 2

A two-year-old boy presented with a painless mass of 4.5 cm at the dorsum of the left foot, that had been increasing in size over several months. On MRI, the mass was located in the subcutaneous tissue, extending into the interosseous muscles between the first and second as well as the second and third metatarsals. The lesion was homogenously hyperintense on T2-weighted (W) images and hypointense on T1W images, with moderate diffusion restriction and homogenous enhancement. There were no metastases present.

Two months after non-radical resection, the patient did not show any signs of residual tumor or recurrence and a wait-and-see policy with close follow-up was chosen.

#### 3.1.3. Case 3

A boy was born with a poorly delineated mass at the right knee.

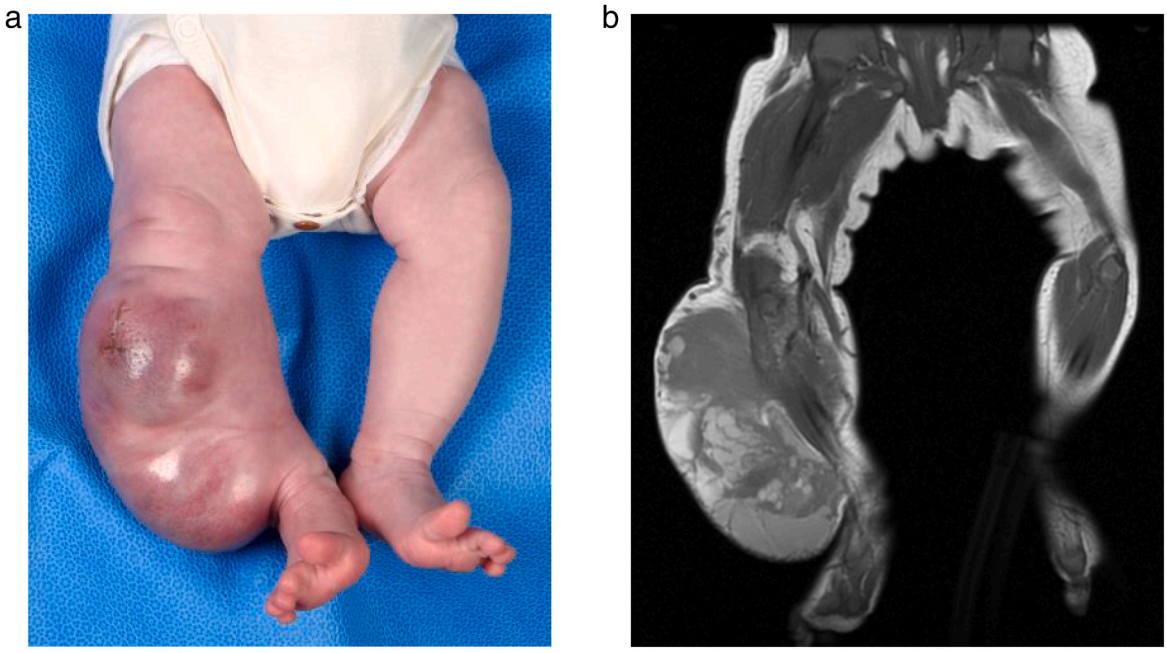


**Fig. 1.** Case 1: a. Clinical picture of the tumor at the right lower leg at presentation. b. MRI imaging of the right lower leg in coronal plane: T1 FSE (Fast spin echo) sequence shows the heterogeneous mass with extensive hemorrhagic components with high T1 signal.

Growth of the lesion paralleled the growth of the child without disproportional progression. MRI showed a diffuse growing lesion of the deep subcutaneous fat of the prepatellar and infrapatellar region with both fatty (hyperintense on T1W images and hypointense on fat-suppressed images) and fibrous (hypointense on T1W and intermediate to hyperintense on T2W images) components. There was homogenous uptake after contrast of the fibrotic component. Cysts were not observed.

Since eight months, the patient is under close follow-up without any further treatment so far.

#### 3.1.4. Case 4

A two-year-old boy was admitted to the hospital due to a large mass involving the upper extremity and shoulder. The tumor was incompletely resected and subsequently chemotherapy was given. The patient is currently alive with no residual disease after five years of follow-up.

### 3.2. Histological features (also depicted in Table 1)

#### 3.2.1. Cases with classic IFS features resembling cellular CMN (cases 1 and 2)

The biopsies of both tumors displayed similar features, resembling classic IFS according to the WHO classification [28]. They consisted of a cellular proliferation with a haphazard (case 1) to bundled (case 2) growth pattern of relatively monomorphic spindle cells with elongated nuclei, inconspicuous nucleoli and scant cytoplasm. Mitoses were abundant. There was only little intervening stroma with multiple dilated blood vessels. Foci of necrosis were observed (Figs. 2 and 3. Table 1). Immunohistochemistry revealed pan-TRK and EGFR positivity.

The resection specimen of case 1 after chemotherapy showed mainly reactive changes consisting of fibrosis, edema and hemosiderin deposition with only little residual tumor (20–30%).

#### 3.2.2. IFS cases with "composite fibromatosis" pattern, resembling classic/mixed CMN (cases 3 and 4)

The biopsy of case 3 contained only a small tumor area within subcutaneous fat. The lesion was hypocellular consisting of a relatively monomorphic spindle cell proliferation, arranged in bundles. The tumor cells showed elongated nuclei, inconspicuous nucleoli and moderate amounts of pale eosinophilic cytoplasm. Mitoses were rare (<2/10 HPF). A collagenous stroma was present as well as some dilated vessels. There was no necrosis (Fig. 4; Table 1). There was too little material for immunohistochemistry. Case 4 showed, in addition to the in case 3 described hypocellular areas, more cellular foci with a herringbone growth pattern, mild pleomorphism and a higher mitotic rate. In these areas, a hemangiopericytoma-like vasculature was present (Table 1). EGFR immunohistochemistry was positive in case 4.

### 3.3. Molecular analyses

No gene fusions were detected by whole transcriptome sequencing (cases 1–3) and NGS Oncomine panel (case 4).

Using WES (cases 1 and 2) a duplication of exons 18–25 of the *EGFR* gene was revealed corresponding to an *EGFR-KDD* (Fig. 5). Closer inspection of the RNA sequencing data of both cases provided proof that this duplication was situated in tandem, confirming duplication of the kinase domain. RNA sequencing data of case 3 were consistent with the same *EGFR-KDD* found in cases 1 and 2. In case 4, the corresponding *EGFR-KDD* was detected by NGS Oncomine panel.

The RNA expression profile of case 1 was highly concordant to a cCMN case harboring an *EGFR-KDD* (score 0.86). Case 2 was classified as an *NTRK1* rearranged sarcoma (score 0.85) based upon gene expression profiling. Case 3 had a lipoblastoma-like gene expression profile (score 0.92), likely due to the prominent adipocytic component in the biopsy compared to tumor tissue and was therefore considered not representative. No RNA expression data were available for case 4. Our two CMN control cases with an *EGFR-KDD* matched with an *NTRK1* rearranged sarcoma (mixed CMN) (score 0.86), and an IFS with an *EGFR-KDD* (cCMN) (score 0.79), respectively. In the context of the entire spectrum of pediatric malignancies collected at the Princess Maxima Center, the expression profile of IFSs and CMNs were highly concordant, regardless of the genetic aberration (*NTRK* translocation versus *EGFR KDD*). In addition, the RNA expression of EGFR was around twice as high in the cases with an *EGFR-KDD* compared to the *NTRK* rearranged tumors.

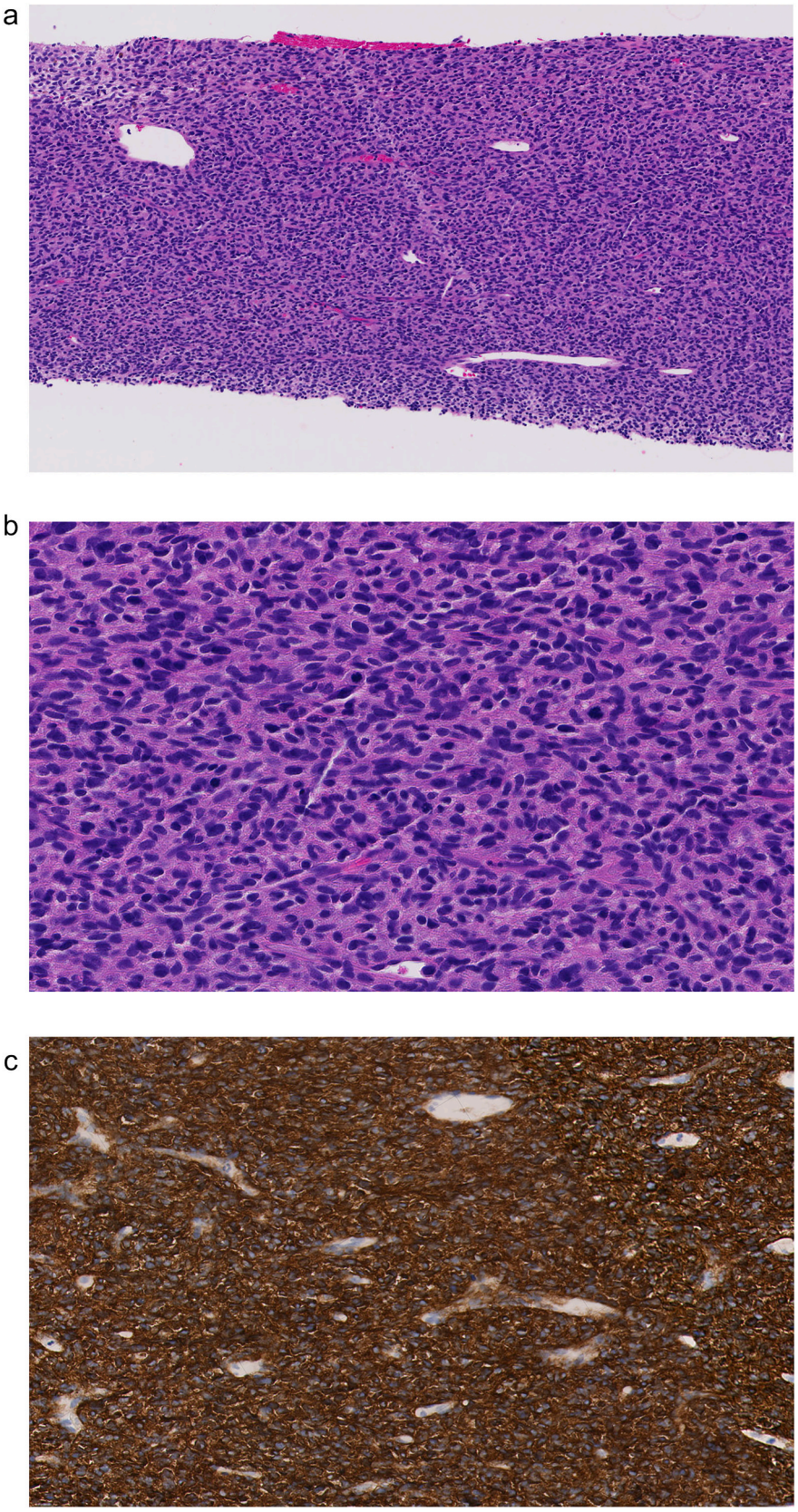


**Fig. 2.** a. Case 1: HE stain of the tumor showing a cellular, monomorphic spindle cell proliferation with a haphazard growth pattern and prominent vasculature. Magnification: 13×.
b. HE stain showing tumor cells with spindled nuclei without prominent nucleoli and little cytoplasm. Multiple mitoses are present. Magnification: 40×.
c. EGFR immunohistochemistry showing diffuse, strong staining of the tumor cells. Magnification: 25×.

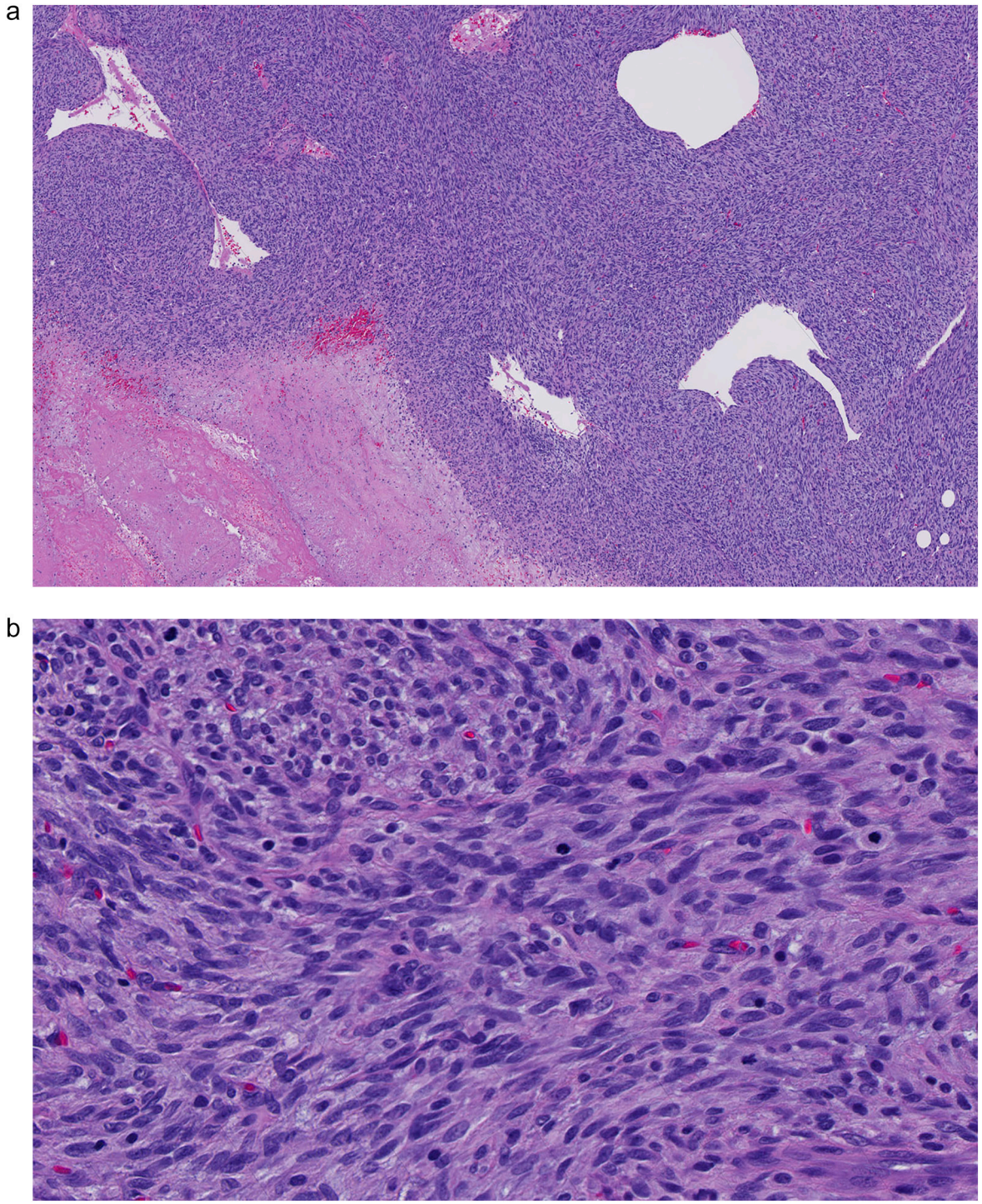


**Fig. 3.** a. Case 2: HE stain showing tumor located in subcutaneous fat. Note multiple dilated vessels and some necrosis. Magnification: 5×.
b. HE stain showing a cellular, monomorphic spindle cell proliferation arranged in bundles, with frequent mitoses. Magnification: 40×.

## 4. Discussion

In this case series we describe four pediatric patients aged 0–2 years, all with tumors on the extremities, clinically, morphologically and immunohistochemically in line with IFS according to the WHO criteria [28]. Molecular analyses did not reveal relevant fusion genes in all of them; in particular no *ETV6-NTRK3* fusion was found. Instead, all cases showed an *EGFR-KDD* as dominant driver mutation with consequently upregulation of the EGFR kinase domain. As in all cases no abnormalities of the kidneys were detected, it was concluded that these tumors represent IFSs instead of unusually metastasized CMNs [10].

While cases 1 and 2 were highly cellular, morphologically in keeping with classic IFS and cCMN, cases 3 and 4 were less cellular and more fibrous, similar to classic/mixed CMN or so called 'composite fibromatosis' [29]. These latter cases might be comparable to the recently described 'lipofibromatosis-like neural tumor' with *NTRK* rearrangement [30]. Thus, it is not surprising that IFS, as part of the *NTRK* fusion family of tumors, shows a broader morphological spectrum.

In CMN, *EGFR-KDD* is already reported as an alternative genetic driver to the *NTRK*-associated fusion genes, also identified in our two

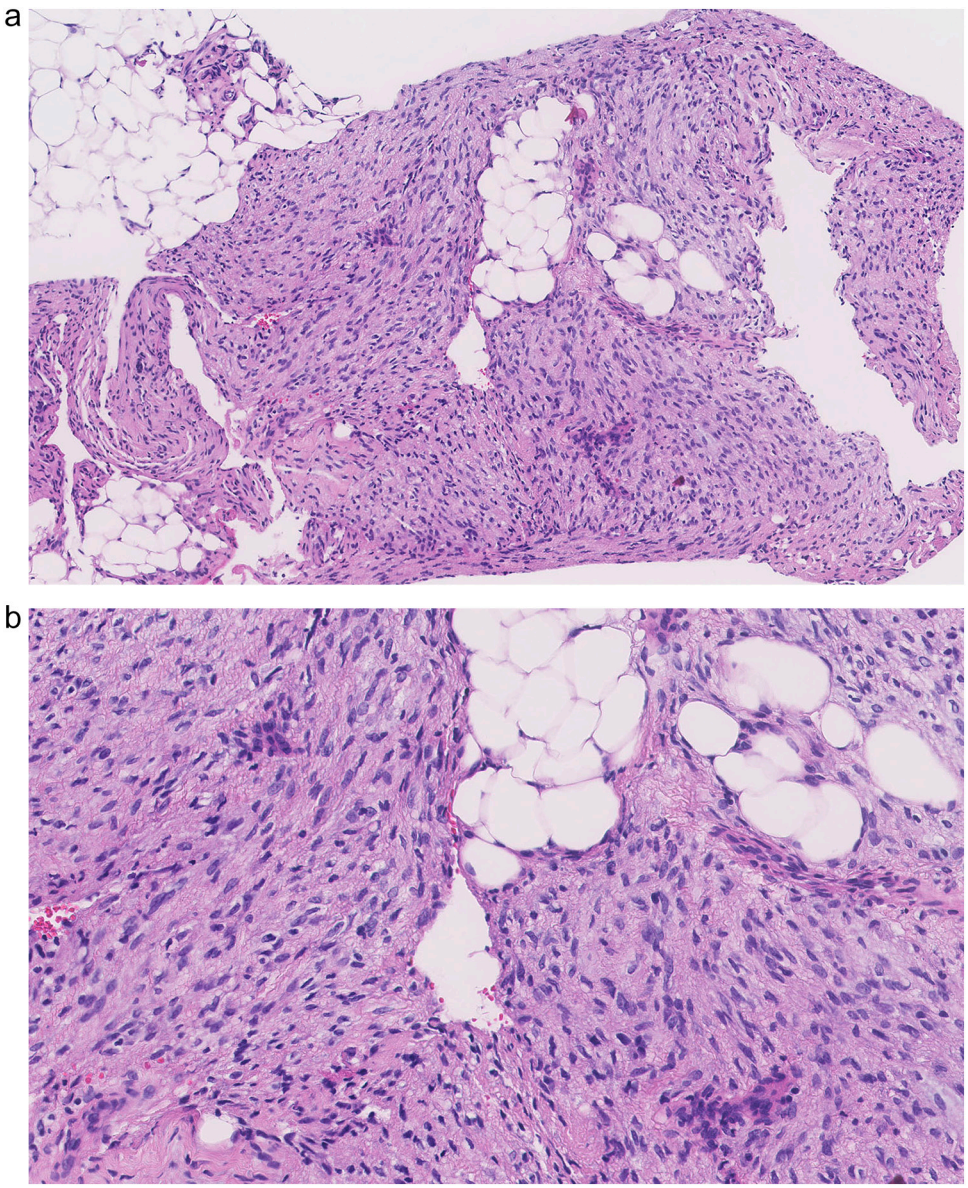


**Fig. 4.** a. Case 3: HE stain showing a hypocellular, monomorphic spindle cell proliferation arranged in bundles between the subcutaneous fat. Magnification: 13×. b. HE stain showing tumor cells with spindled nuclei without prominent nucleoli and with eosinophilic cytoplasm. Magnification: 25×.

**Table 1**
Histological features of the four cases.

| Case | Morphology |
|---|---|
| 1 and 2: resembling classic IFS/ cCMN | Hypercellular; monomorphic spindle cells; haphazard to bundled growth pattern; little stroma; dilated vessels; necrosis; multiple mitoses |
| 3 and 4: resembling 'composite fibromatosis'/classic-mixed CMN | Hypocellular; monomorphic spindle cells; bundled growth pattern; collagenous stroma; dilated vessels; no necrosis; few mitoses |

Abbreviations: IFS: cCMN: cellular congenital mesoblastic nephroma; infantile fibrosarcoma.

CMN cases without a fusion gene [15,17,18]. This further supports the hypothesis that IFS and CMN are similar tumors at different locations.

In one study, 26 IFSs were analyzed for *ETV6-NTRK3* and *EGFR-KDD* using RT-PCR. A fusion transcript was found in 70% of the lesions but none of the cases harbored an *EGFR-KDD*. In contrast, in the same study *EGFR-KDD* positive tumors were prevalent among all CMN subtypes, most often in mixed and classic CMNs [22]. Also, *BRAF*, *NTRK1*, *ALK* and *RET* fusions were detected as alternative genetic aberrations in both CMN and IFS, further strengthening that these entities are very closely related and driven by hyperactivated receptor protein kinase signaling [22,31-33].

Another study showed *EGFR-KDDs* in different tumor types, including an unclassified sarcoma of a 27-year-old female. Possibly, this represents the first report of an *NTRK*-family associated soft tissue tumor harboring the alternative *EGFR-KDD* [34].

Constitutive activation of the mentioned tyrosine or serine/threonine kinases confers oncogenic potential and is the driver mutation in IFS, CMN and the other (soft tissue) tumors of this category [22,30-33]. Whereas *NTRK* activation is due to in-frame fusions of the kinase domain to the 5′ region of a partner gene, EGFR activation is based upon the duplication of the kinase domain, with both mechanisms resulting in high levels of autophosphorylation [35,36]. The NTRK fusion protein results in upregulation of both the Phosphatidylinositol-3′kinase (PI3K)-AKT pathway and the Ras-mitogen-activated protein kinase (MAPK) pathway [3]. *EGFR-KDD* also activates the MAPK pathway and thereby

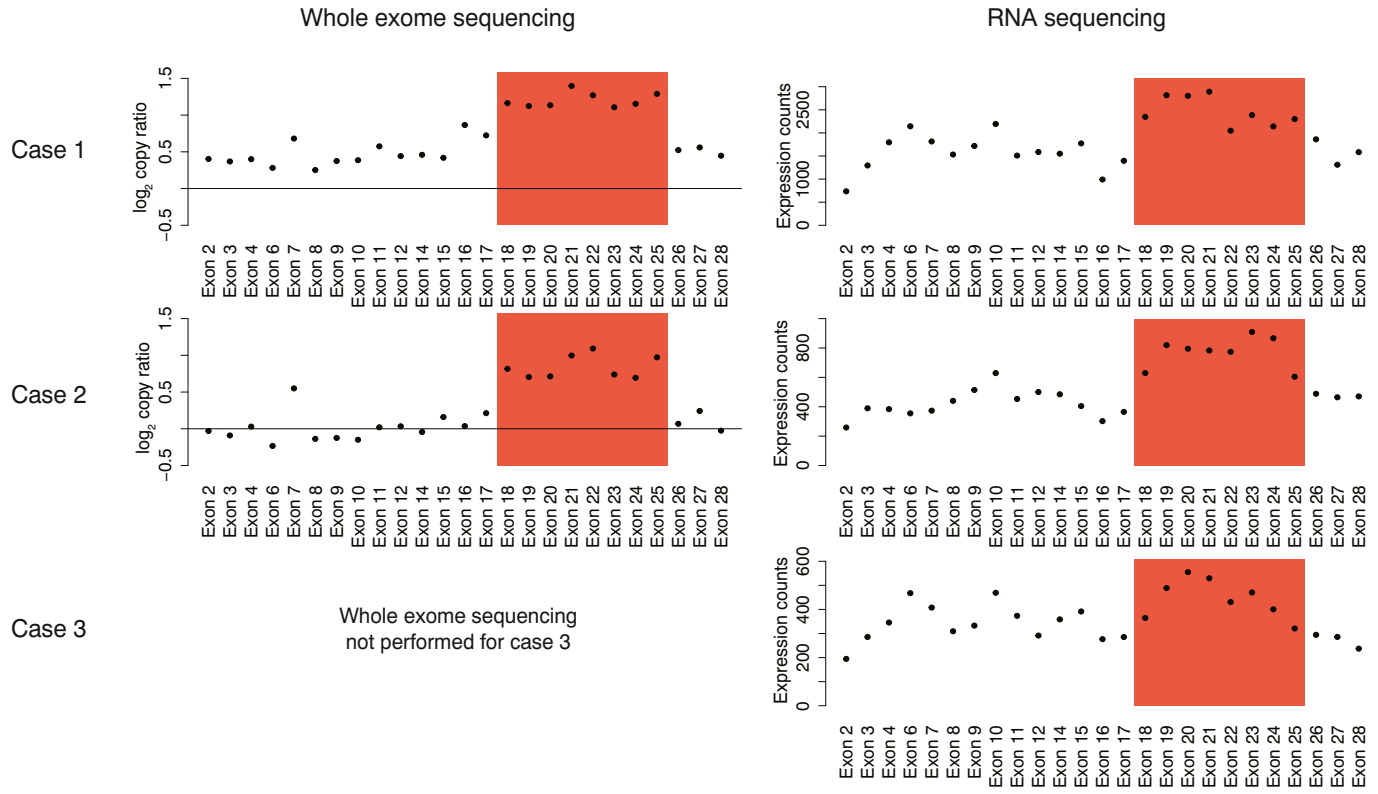


**Fig. 5.** Exon copy ratio and expression counts of EGFR kinase domain duplication.
Whole exome sequencing copy ratio and expression counts for individual EGFR exons. EGFR kinase domain is highlighted in red. Whole exome sequencing copy ratios are higher for exons 18 to 25 (EGFR kinase domain), indicating the duplication. The effect is less clear in the expression counts, however all cases show sequencing reads for which the 5' end maps to exon 25 en the 3' end to exon 18, thereby confirming the direct connection of exon 25 to exon 18.

equally drives uncontrolled cell proliferation [35-37].

Although the genetic alterations of *NTRK* (rearrangements) and *EGFR* (*KDD*) are clearly different, the downstream effect of the activated tyrosine kinases seems to be analogous [3,30]. This is also reflected by our highly similar RNA expression profiles of IFS, CMN and other *NTRK*-related lesions, regardless of the genetic aberration (*NTRK* rearrangement versus *EGFR KDD*). These findings explain that other genetic mechanisms, in particular tandem repeat duplications of the kinase domain of receptor tyrosine kinases, can function as an alternative to gene fusions in fusion driven sarcomas, analogous to the *FGFR1-KDDs* found in pilocytic astrocytomas lacking a *BRAF* rearrangement and *MET-KDDs* found in lung cancer [38-40]. Besides *KDDs*, alternative tandem repeat duplications can also occur in other fusion gene-associated tumors, like *BCOR internal tandem duplications* in BCOR sarcomas [38].

The *EGFR* expression on RNA level was around twice as high in our IFS cases with an *EGFR KDD* (cases 1–3) compared to the group of *NTRK* rearranged sarcomas. This is in agreement with our EGFR immunohistochemical results with positivity in three of the cases. Thus, EGFR immunohistochemistry could be a good surrogate marker of *EGFR* alterations in cases suspicious for IFS (or other *NTRK*-related soft tissue tumors), including those with 'composite fibromatosis' morphology lacking a gene fusion, and/or being negative for pan-TRK immunohistochemistry. Attention needs to be paid though regarding its specificity, as has previously been mentioned in literature [19,21]. Indeed, in two of our classic IFS cases with an *NTRK3* rearrangement EGFR immunohistochemistry was weakly and strongly positive, respectively (data not shown).

Clinical response to EGFR targeted therapy has been described in lung carcinomas harboring an *EGFR-KDD* [4,34]. Although there is no experience yet with CMN or IFS, this might be promising in the future for patients with extensive disease lacking a fusion gene [19,21].

As follow-up was limited in our cases, it is not possible to indicate the prognostic value of the presence of an *EGFR-KDD* in comparison to *NTRK* fusions in IFS. In a recent case series of CMN, it was shown that all classic and mixed subtypes with an *EGFR-KDD* had no evidence of disease at last follow-up. However, this is not different from the *NTRK* rearranged lesions, and it should be noted that CMNs have a good prognosis in most cases [2,19]. The only case that depicted more aggressive behavior was a retroperitoneal tumor with involvement of the kidney, classified as mixed CMN, still receiving chemotherapy after 48 months of follow-up. However, it seems logical that retroperitoneal location (outside the kidney) represents the most important parameter for this relatively aggressive clinical course [19].

In conclusion, we have described for the first time the presence of *EGFR-KDDs* as driver mutation in IFS, alternatively to an *NTRK* fusion gene. This reinforces the assumption that IFS and CMN are closely related tumors with a similar morphological spectrum, with some IFS cases resembling cCMN while others are akin to classic/mixed CMN. This is in accordance with the broad spectrum of *NTRK*- (and other protein kinase) related lesions in general [30]. Future studies are required to confirm our findings with correlation to morphology and prognosis of *EGFR-KDD* related lesions, as well as the possible role of targeted therapy against EGFR in these tumors. As other tandem repeat duplications are an alternative genetic mechanism in other fusion gene associated tumors as well, such as *BCOR* sarcomas, this should be kept in mind when a fusion gene is absent.

## Funding

This research received no specific grant from any funding agency in the public, commercial, or not-for-profit sectors.

## Declaration of competing interest

The Authors declare that there is no conflict of interest.

## References


[1] Orbach D, Rey A, Cecchetto G, Oberlin O, Casanova M, Thebaud E, et al. Infantile fibrosarcoma: management based on the European experience. J Clin Oncol 2010;28(2):318–23.
[2] Gooskens SL, Houwing ME, Vujanic GM, Dome JS, Diertens T, Coulomb-l'Hermine A, et al. Congenital mesoblastic nephroma 50 years after its recognition: a narrative review. Pediatr Blood Cancer 2017;64(7).
[3] Morrison KB, Tognon CE, Garnett MJ, Deal C, Sorensen PH. ETV6-NTRK3 transformation requires insulin-like growth factor 1 receptor signaling and is associated with constitutive IRS-1 tyrosine phosphorylation. Oncogene 2002;21(37):5684–95.
[4] Du Z, Brown BP, Kim S, Ferguson D, Pavlick DC, Jayakumaran G, et al. Structure-function analysis of oncogenic EGFR kinase domain duplication reveals insights into activation and a potential approach for therapeutic targeting. Nat Commun 2021;12(1):1382.
[5] Orbach D, Brennan B, De Paoli A, Gallego S, Mudry P, Francotte N, et al. Conservative strategy in infantile fibrosarcoma is possible: the European paediatric soft tissue sarcoma study group experience. Eur J Cancer 2016;57:1–9.
[6] Gupta A, Sharma S, Mathur S, Yadav DK, Gupta DK. Cervical congenital infantile fibrosarcoma: a case report. J Med Case Rep 2019;13(1):41.
[7] Orbach D, Sparber-Sauer M, Laetsch TW, Minard-Colin V, Bielack SS, Casanova M, et al. Spotlight on the treatment of infantile fibrosarcoma in the era of neurotrophic tropomyosin receptor kinase inhibitors: international consensus and remaining controversies. Eur J Cancer 2020;137:183–92.
[8] Bender J, Anderson B, Bloom DA, Rabah R, McDougall R, Vats P, et al. Refractory and metastatic infantile fibrosarcoma harboring LMNA-NTRK1 fusion shows complete and durable response to crizotinib. Cold Spring Harb Mol Case Stud 2019;5(1).
[9] Wang ZP, Li K, Dong KR, Xiao XM, Zheng S. Congenital mesoblastic nephroma: clinical analysis of eight cases and a review of the literature. Oncol Lett 2014;8(5):2007–11.
[10] Jehangir S, Kurian JJ, Selvarajah D, Thomas RJ, Holland AJA. Recurrent and metastatic congenital mesoblastic nephroma: where does the evidence stand? Pediatr Surg Int 2017;33(11):1183–8.
[11] Rubin BP, Chen CJ, Morgan TW, Xiao S, Grier HE, Kozakewich HP, et al. Congenital mesoblastic nephroma t(12;15) is associated with ETV6-NTRK3 gene fusion: cytogenetic and molecular relationship to congenital (infantile) fibrosarcoma. Am J Pathol 1998;153(5):1451–8.
[12] Marsden HB, Newton Jr WA. New look at mesoblastic nephroma. J Clin Pathol 1986;39(5):508–13.
[13] Bolande RP. Congenital mesoblastic nephroma of infancy. Perspect Pediatr Pathol 1973;1:227–50.
[14] Bolande RP, Brough AJ, Izant Jr RJ. Congenital mesoblastic nephroma of infancy. A report of eight cases and the relationship to Wilms' tumor. Pediatrics 1967;40(2):272–8.
[15] Richmond H, Dougall AJ. Neonatal renal tumors. J Pediatr Surg 1970;5(4):413–8.
[16] Wigger HJ. Fetal hamartoma of kidney. A benign, symptomatic, congenital tumor, not a form of Wilms' tumor. Am J Clin Pathol 1969;51(3):323–37.
[17] Knezevich SR, Garnett MJ, Pysher TJ, Beckwith JB, Grundy PE, Sorensen PH. ETV6-NTRK3 gene fusions and trisomy 11 establish a histogenetic link between mesoblastic nephroma and congenital fibrosarcoma. Cancer Res 1998;58(22):5046–8.
[18] Church AJ, Calicchio ML, Nardi V, Skalova A, Pinto A, Dillon DA, et al. Recurrent EML4-NTRK3 fusions in infantile fibrosarcoma and congenital mesoblastic nephroma suggest a revised testing strategy. Mod Pathol 2018;31(3):463–73.
[19] Lei L, Stohr BA, Berry S, Lockwood CM, Davis JL, Rudzinski ER, et al. Recurrent EGFR alterations in NTRK3 fusion negative congenital mesoblastic nephroma. Pract Lab Med 2020;21:e00164.
[20] Anderson J, Gibson S, Sebire NJ. Expression of ETV6-NTRK in classical, cellular and mixed subtypes of congenital mesoblastic nephroma. Histopathology 2006;48(6):748–53.
[21] Zhao M, Yin M, Kuick CH, Chen H, Aw SJ, Merchant K, et al. Congenital mesoblastic nephroma is characterised by kinase mutations including EGFR internal tandem duplications, the ETV6-NTRK3 fusion, and the rare KLHL7-BRAF fusion. Histopathology 2020;77(4):611–21.
[22] Wegert J, Vokuhl C, Collord G, Del Castillo Velasco-Herrera M, Farndon SJ, Guzzo C, et al. Recurrent intragenic rearrangements of EGFR and BRAF in soft tissue tumors of infants. Nat Commun 2018;9(1):2378.
[23] Rossi S, Barresi S, Stracuzzi A, Lopez-Nunez O, Chiaravalli S, Ferrari A, et al. DICER1-associated malignancies mimicking germ cell neoplasms: report of two cases and review of the literature. Pathol Res Pract 2021;225:153553.
[24] Hehir-Kwa. Accepted for publication. 2021.
[25] Andrews S. FastQC. 2015.
[26] Institute B. Picard toolkit. Available from: http://broadinstitute.github.io/picard/; 2019.
[27] Dobin A, Davis CA, Schlesinger F, Drenkow J, Zaleski C, Jha S, et al. STAR: ultrafast universal RNA-seq aligner. Bioinformatics 2013;29(1):15–21.
[28] IARC. WHO Classification of Tumours Soft Tissue and Bone Tumours. 5th edition3; 2020.
[29] Alaggio R, Barisani D, Ninfo V, Rosolen A, Coffin CM. Morphologic overlap between infantile myofibromatosis and infantile fibrosarcoma: a pitfall in diagnosis. Pediatr Dev Pathol 2008;11(5):355–62.
[30] Antonescu CR. Emerging soft tissue tumors with kinase fusions: an overview of the recent literature with an emphasis on diagnostic criteria. Genes Chromosomes Cancer 2020;59(8):437–44.
[31] Kao YC, Fletcher CDM, Alaggio R, Wexler L, Zhang L, Sung YS, et al. Recurrent BRAF gene fusions in a subset of pediatric spindle cell sarcomas: expanding the genetic Spectrum of tumors with overlapping features with infantile fibrosarcoma. Am J Surg Pathol 2018;42(1):28–38.
[32] Tan SY, Al-Ibraheemi A, Arhens WA, Oesterheld JE, Fanburg-Smith JC, Liu YJ, et al. ALK rearrangements in infantile fibrosarcoma-like spindle cell tumors of soft tissue and kidney. Histopathology 2021.
[33] Davis JL, Vargas SO, Rudzinski ER, Lopez Marti JM, Janeway K, Forrest S, et al. Recurrent RET gene fusions in paediatric spindle mesenchymal neoplasms. Histopathology 2020;76(7):1032–41.
[34] Gallant JN, Sheehan JH, Shaver TM, Bailey M, Lipson D, Chandramohan R, et al. EGFR kinase domain duplication (EGFR-KDD) is a novel oncogenic driver in lung cancer that is clinically responsive to afatinib. Cancer Discov 2015;5(11):1155–63.
[35] Somwar R, Hofmann NE, Smith B, Odintsov I, Vojnic M, Linkov I, et al. NTRK kinase domain mutations in cancer variably impact sensitivity to type I and type II inhibitors. Commun Biol 2020;3(1):776.
[36] Maruyama IN. Mechanisms of activation of receptor tyrosine kinases: monomers or dimers. Cells 2014;3(2):304–30.
[37] Katz M, Amit I, Yarden Y. Regulation of MAPKs by growth factors and receptor tyrosine kinases. Biochim Biophys Acta 2007;1773(8):1161–76.
[38] Roy A, Kumar V, Zorman B, Fang E, Haines KM, Doddapaneni H, et al. Recurrent internal tandem duplications of BCOR in clear cell sarcoma of the kidney. Nat Commun 2015;6:8891.
[39] Wang B, Yu R, Ou Q, Bao H, Wu X, Shao Y, et al. Identification of kinase domain duplications across diverse cancer types in Chinese population by comprehensive genomic profiling (CGP). J Clin Oncol 2020;38(15_suppl):e13522.
[40] Jones DTW. Recurrent somatic alterations of FGFR1 and NTRK2 in pilocytic astrocytoma. Nat Genet 2013;45(8).